

A COLLOCATION HEAT POLYNOMIALS METHOD FOR ONE-DIMENSIONAL INVERSE STEFAN PROBLEMS

ORAZBEK NARBEEK, SAMAT A. KASSABEK, AND TARGYN NAURYZ

ABSTRACT. The inverse one-phase Stefan problem in one dimension, aimed at identifying the unknown time-dependent heat flux $P(t)$ with a known moving boundary position $s(t)$, is investigated. A previous study [16] attempted to reconstruct the unknown heat flux $P(t)$ using the Variational Heat Polynomials Method (VHPM). In this paper, we develop the Collocation Heat Polynomials Method (CHPM) for the reconstruction of the time-dependent heat flux $P(t)$. This method constructs an approximate solution as a linear combination of heat polynomials, which satisfies the heat equation, with the coefficients determined using the collocation method. To address the resulting ill-posed problem, Tikhonov regularization is applied. As an application, we demonstrate the effectiveness of the method on benchmark problems. Numerical results show that the proposed method accurately reconstructs the time-dependent heat flux $P(t)$, even in the presence of significant noise. The results are also compared with those obtained in [16] using the VHPM.

1. INTRODUCTION

The heat polynomials $v_n(x, t)$ were introduced by Appell in 1892 [2] as the coefficients of the generating function:

$$g(x, t, z) = e^{xz+ta^2z^2},$$

where the function $g(x, t, z)$ satisfies the heat equation $g_t - a^2g_{xx} = 0$ for any value of z . This function can be expanded in powers of z using a Taylor series:

$$g(x, t, z) = \sum_{n=0}^{\infty} v_n(x, t)z^n.$$

Rosenbloom and Widder, in their series of works [37], [42] - [46], along with Haimo [12], investigated the expansion of solutions $u(x, t)$ to the heat equation

$$(1) \quad \frac{\partial u}{\partial t} = a^2 \frac{\partial^2 u}{\partial x^2},$$

using heat polynomials $v_n(x, t)$. These polynomials are given by the expression:

$$(2) \quad v_n(x, t) = \sum_{m=0}^{\lfloor n/2 \rfloor} \frac{a^{2m}n!}{m!(n-2m)!} x^{n-2m} t^m.$$

It is evident that this linear combination of heat polynomials also satisfies the heat equation (1).

The core idea behind this method is to construct exact analytical or approximate solutions to the problem as a linear combination of the polynomials in (2), much like in the Trefftz method [39], where unknown coefficients are determined from initial and boundary conditions. This approach has been further developed in the works of Yano [47], Futakiewicz [4], Hozejowski [13], and Grysa [6].

2010 *Mathematics Subject Classification.* 80A22, 80A23, 80M30, 35C11.

Key words and phrases. Inverse Stefan problems, approximate solution, heat polynomials method, moving boundary.

The authors were supported by the grant AP19675480 "Problems of heat conduction with a free boundary arising in modeling of switching processes in electrical devices".

Numerous studies have explored the application of the heat polynomial method (HPM) and the Trefftz method for various heat conduction problems on fixed domains, see e.g., [7] - [9], [28] - [31]. However, the literature on applying HPM to heat problems with moving boundaries is relatively scarce; see [16] - [20], [23, 25, 36].

Heat conduction problems with moving boundaries and phase transitions, known as Stefan problems, arise in various real-world and engineering applications, such as melting, welding, freezing, and cooling [11, 38]. The direct Stefan problem involves determining the temperature distribution and the position of a moving boundary over time, given the heat flux or boundary conditions. This problem typically models processes where phase change, such as melting or evaporation, drives the movement of the boundary. In contrast, inverse Stefan problem focuses on identifying unknown parameters, such as the time-dependent heat flux or the boundary's position, based on known temperature data or other boundary conditions [5]. Due to its ill-posed nature, this problem is more complex and commonly encountered in situations where direct measurements are challenging. An example of a real-world application of the inverse Stefan problem is in determining the heat flux components in low-voltage electric arc systems [24]. This is particularly relevant since experimental methods for measuring heat fluxes can often result in significant errors, making the use of inverse methods highly valuable.

Many studies have addressed inverse Stefan problems [3], [10], [14] - [21], [35], [36]. One effective method for solving these problems is the heat potential method, which reduces boundary value problems to integral equations. However, when the domain is degenerate at the initial time, singularities in these integral equations introduce additional difficulties. Numerical methods like finite difference and finite element techniques [34, 48] are widely used but can be computationally expensive, especially when fine discretization is required. To overcome these limitations, meshless methods [15] and method of fundamental solutions [14] have been developed. While flexible, these methods often face stability and convergence issues, particularly with noisy data. The slow convergence of many iterative methods and the need for accurate solutions with low computational cost have motivated this study. We aim to improve the efficiency and stability of inverse one-phase Stefan problem solutions using the CHPM, which addresses several of these limitations.

The collocation method has gained prominence as an effective and versatile tool for solving inverse heat conduction problems (IHCPs) and Stefan problems. Unlike traditional mesh-based methods, the collocation method employs radial basis functions or other approximating functions to solve partial differential equations without the necessity of a predefined mesh. This meshless approach provides significant flexibility, especially when dealing with complex geometries and irregular domains, while simultaneously reducing computational costs associated with mesh generation [22]. Over time, the collocation method has evolved to include various regularization techniques aimed at addressing the ill-conditioning that typically arises in inverse problems, particularly IHCPs, where small errors in data can lead to large errors in solutions [33]. For example, recent advancements such as the local meshless methods [41] and physics-informed neural networks (PINNs) [49] have further extended the capabilities of the collocation method for complex multi-layered media and nonlinear heat conduction problems, offering promising solutions to both forward and inverse problems. These developments have significantly enhanced the stability and accuracy of the method, making it an increasingly popular approach for tackling one-phase Stefan problems [22, 33, 40].

In this article, we present the approximate solutions of one-phase inverse Stefan problems, focusing on the development of a novel collocation heat polynomials method. The primary contribution of this work lies in the application of CHPM for solving inverse Stefan problems, offering an efficient and accurate alternative to existing methods. Our goal in this series of studies [16] - [20] is to create and refine an approximate method that can effectively handle Stefan-type problems. To demonstrate the method's efficacy and investigate the convergence of the approximate solutions, we apply CHPM to two numerical examples, illustrating its potential as a robust tool for inverse Stefan problems.

The paper is organized as follows. Formulation of the one-dimensional inverse Stefan problems are presented in Section 2. In Section 3, we give a brief sketch of the heat polynomials method

to solve the Stefan type problems. In Section 4, we consider an application of the CHPM to two numerical examples. In order to investigate the stability of the approximate solution, random additive noise is added to the input data. Summary and Concluding remarks are discussed briefly in Section 5.

2. ONE-PHASE STEFAN PROBLEM

Consider the following one-dimensional, one-phase Stefan problem:

$$(3) \quad \frac{\partial u}{\partial t} = a^2 \frac{\partial^2 u}{\partial x^2} \quad \text{in } 0 < x < s(t), \quad 0 < t \leq T,$$

where a represents the thermal diffusivity, and $s(t) > 0$ is a free boundary that is assumed to be a sufficiently smooth function. The heat conduction domain is defined as $D = (0, s(t)) \times (0, T)$, with its closure given by $\bar{D} = [0, s(t)] \times [0, T]$.

The initial condition is provided as:

$$(4) \quad u(x, 0) = f(x), \quad 0 \leq x \leq s(0),$$

with Neumann boundary conditions specified as:

$$(5) \quad -\lambda \frac{\partial u(0, t)}{\partial x} = P(t), \quad 0 < t \leq T,$$

and Dirichlet and Stefan conditions imposed on the moving boundary $x = s(t)$:

$$(6) \quad u(s(t), t) = u^*, \quad 0 < t \leq T,$$

$$(7) \quad -\lambda \frac{\partial u(x, t)}{\partial x} \Big|_{x=s(t)} = L\gamma \frac{ds(t)}{dt}, \quad 0 < t \leq T,$$

along with the initial condition on the moving boundary:

$$(8) \quad s(0) = s_0.$$

For the direct one-phase Stefan problem, we seek to determine the free boundary $x = s(t) \in C^1([0, T])$ and the unknown temperature distribution $u(x, t) \in C^2(D) \cap C^1(\bar{D})$, which satisfy Eqs. (3), (4), (5), (6), (7), and (8). The parameters a , λ , u^* , L , γ , $f(x)$, $P(t)$, and s_0 are assumed to be known.

Unlike the direct Stefan problem, numerous variations of inverse Stefan problems can be defined. In this paper, we focus on investigating a classical inverse Stefan problem where the Neumann boundary condition at $x = 0$ is not prescribed and must be reconstructed, along with the temperature distribution, assuming the position of the moving boundary $s(t)$ is known a priori.

3. THE COLLOCATION HEAT POLYNOMIALS METHOD

In this study, we employ the collocation heat polynomials method to solve the inverse one-phase Stefan problem. This method approximates the temperature distribution and heat flux at the moving boundary using a linear combination of heat polynomials, which inherently satisfy the heat equation. The Stefan problem is transformed into a system of algebraic equations by applying the boundary and initial conditions through integration.

We approximate the temperature distribution $u(x, t)$ as a linear combination of heat polynomials:

$$(9) \quad u(x, t) = \sum_{n=0}^N c_n v_n(x, t), \quad 0 \leq x \leq s(t), \quad 0 \leq t \leq T$$

where $v_n(x, t)$ represents the n^{th} -order heat polynomials. These polynomials satisfy the heat equation, and the coefficients c_n are unknown and determined through the collocation process.

To determine these coefficients, we apply the collocation method by enforcing the boundary and initial conditions through an integration approach over finite intervals. Instead of evaluating

the conditions at discrete points, we integrate the residuals over the intervals, making the system more stable for ill-posed problems.

At the moving boundary $x = s(t)$, we integrate the Dirichlet and Neumann conditions over time intervals $(t_{i-1}, t_i]$, for $i = 1, 2, \dots, M$, as follows:

$$\int_{t_{i-1}}^{t_i} [u(s(t), t) - u^*] dt = \int_{t_{i-1}}^{t_i} \left[\sum_{n=0}^N c_n v_n(s(t), t) - u^* \right] dt = 0,$$

and for the Neumann condition, we have:

$$\int_{t_{i-1}}^{t_i} \left[-\lambda \frac{\partial u}{\partial x} \Big|_{x=s(t)} - L\gamma \frac{ds(t)}{dt} \right] dt = \int_{t_{i-1}}^{t_i} \left[-\sum_{n=0}^N c_n \lambda \frac{\partial v_n(x, t)}{\partial x} \Big|_{x=s(t)} - L\gamma \frac{ds(t)}{dt} \right] dt = 0.$$

The initial condition $u(x, 0) = f(x)$ is handled similarly. We divide the spatial domain $[0, s(0)]$ into N_x intervals and integrate the residuals over each interval:

$$\int_{x_{j-1}}^{x_j} [u(x, 0) - f(x)] dx = \int_{x_{j-1}}^{x_j} \left[\sum_{n=0}^N c_n v_n(x, 0) - f(x) \right] dx = 0.$$

These integrals result in a system of $N \times N$ algebraic equations that can be written in matrix form as:

$$(10) \quad \mathbf{A}\mathbf{c} = \mathbf{b},$$

where \mathbf{A} contains coefficients derived from the integrals, \mathbf{c} is the vector of unknown coefficients c_n , and \mathbf{b} contains the results from the integrated boundary and initial conditions.

The system of equations obtained is often ill-conditioned, meaning that small perturbations in the data can lead to significant errors in the solution [1]. To address this, we apply Tikhonov regularization, modifying the system of equations to:

$$(\mathbf{A}^T \mathbf{A} + \beta I)\mathbf{c} = \mathbf{A}^T \mathbf{b},$$

where \mathbf{A}^T is the transpose of \mathbf{A} , I is the identity matrix, and β is the regularization parameter. This regularization helps to stabilize the solution by controlling the balance between fitting the data and maintaining numerical stability. In our numerical examples, we explore the effect of varying the regularization parameter β on the accuracy of the reconstructed heat flux.

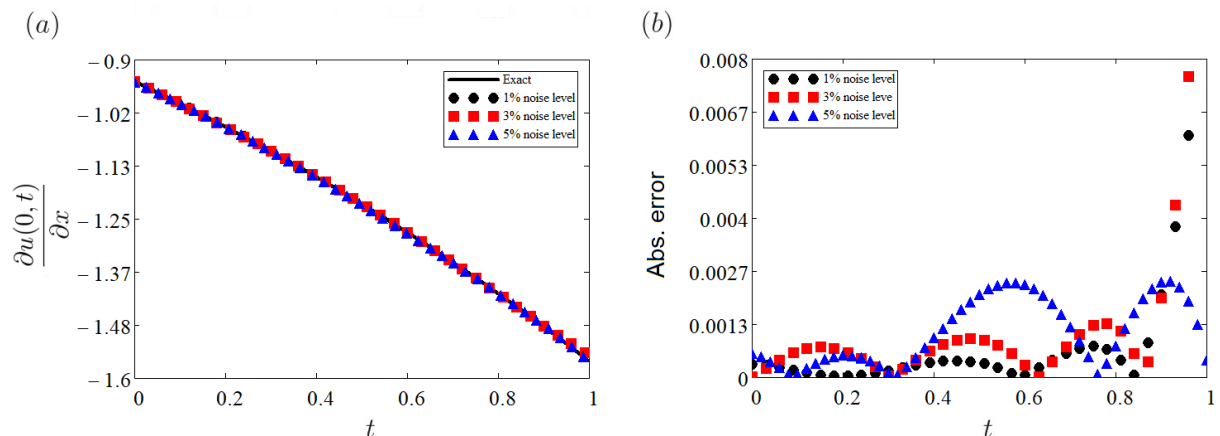


FIGURE 1. (a) For Example 4.1 of the inverse Stefan problem (a) depicts the comparison between the exact and approximate solutions of $u_x(0, t)$, (b) illustrates the absolute error between the exact solution and $u_x(0, t)$ for different noise levels for $N = 12$.

TABLE 1. The values ΔP of the relative error depending on the parameters N and β with zero noise, Example 4.1.

$\beta \setminus N$	4	6	8	10	12	14	16	18	20
0	0.018	$1.90 \cdot 10^{-3}$	$1.08 \cdot 10^{-4}$	$5.06 \cdot 10^{-6}$	$1.71 \cdot 10^{-7}$	$5.06 \cdot 10^{-9}$	$6.57 \cdot 10^{-11}$	$1.67 \cdot 10^{-11}$	$2.05 \cdot 10^{-11}$
$1 \cdot 10^{-13}$	0.018	$1.91 \cdot 10^{-3}$	$1.08 \cdot 10^{-4}$	$5.36 \cdot 10^{-6}$	$2.76 \cdot 10^{-6}$	$2.61 \cdot 10^{-6}$	$3.08 \cdot 10^{-6}$	$2.40 \cdot 10^{-6}$	$2.97 \cdot 10^{-6}$
$1 \cdot 10^{-12}$	0.018	$1.91 \cdot 10^{-3}$	$1.08 \cdot 10^{-4}$	$9.8 \cdot 10^{-6}$	$7.33 \cdot 10^{-6}$	$7.08 \cdot 10^{-6}$	$7.44 \cdot 10^{-6}$	$6.93 \cdot 10^{-6}$	$7.16 \cdot 10^{-6}$
$1 \cdot 10^{-11}$	0.018	$1.91 \cdot 10^{-3}$	$1.10 \cdot 10^{-4}$	$2.85 \cdot 10^{-5}$	$2.54 \cdot 10^{-5}$	$2.16 \cdot 10^{-5}$	$2.03 \cdot 10^{-5}$	$2.02 \cdot 10^{-5}$	$2.06 \cdot 10^{-5}$
$1 \cdot 10^{-10}$	0.018	$1.91 \cdot 10^{-3}$	$1.23 \cdot 10^{-4}$	$6.69 \cdot 10^{-5}$	$6.42 \cdot 10^{-5}$	$6.28 \cdot 10^{-5}$	$7.28 \cdot 10^{-5}$	$6.28 \cdot 10^{-5}$	$7.40 \cdot 10^{-5}$
$1 \cdot 10^{-9}$	0.018	$1.92 \cdot 10^{-3}$	$2.28 \cdot 10^{-4}$	$1.85 \cdot 10^{-4}$	$1.76 \cdot 10^{-4}$	$1.75 \cdot 10^{-4}$	$1.86 \cdot 10^{-4}$	$1.79 \cdot 10^{-4}$	$1.89 \cdot 10^{-4}$
$1 \cdot 10^{-8}$	0.018	$2.01 \cdot 10^{-3}$	$5.84 \cdot 10^{-4}$	$5.75 \cdot 10^{-4}$	$5.16 \cdot 10^{-4}$	$5.14 \cdot 10^{-4}$	$5.29 \cdot 10^{-4}$	$5.32 \cdot 10^{-4}$	$5.59 \cdot 10^{-4}$
$1 \cdot 10^{-7}$	0.018	$2.74 \cdot 10^{-3}$	$1.57 \cdot 10^{-3}$	$1.53 \cdot 10^{-3}$	$1.57 \cdot 10^{-3}$	$1.62 \cdot 10^{-3}$	$1.79 \cdot 10^{-3}$	$1.69 \cdot 10^{-3}$	$1.87 \cdot 10^{-3}$
$1 \cdot 10^{-6}$	0.016	$5.45 \cdot 10^{-3}$	$4.61 \cdot 10^{-3}$	$4 \cdot 10^{-3}$	$4.1 \cdot 10^{-3}$	$4.25 \cdot 10^{-3}$	$4.49 \cdot 10^{-3}$	$4.5 \cdot 10^{-3}$	$4.75 \cdot 10^{-3}$
$1 \cdot 10^{-5}$	0.009	0.011	0.011	0.011	0.012	0.013	0.014	0.014	0.015
$1 \cdot 10^{-4}$	0.05	0.034	0.033	0.035	0.038	0.04	0.044	0.044	0.047
$1 \cdot 10^{-3}$	0.092	0.096	0.097	0.106	0.115	0.124	0.131	0.14	0.146

TABLE 2. The condition number $C(\mathbf{A}_N, \beta)$ depending on the parameters N and β with zero noise, Example 4.1.

$\beta \setminus N$	4	6	8	10	12	14	16	18	20
0	266.57	$2.27 \cdot 10^3$	$2.45 \cdot 10^4$	$4.86 \cdot 10^5$	$1.44 \cdot 10^7$	$5.25 \cdot 10^8$	$1.69 \cdot 10^{10}$	$1.69 \cdot 10^{10}$	$3.22 \cdot 10^{13}$
$1 \cdot 10^{-13}$	266.57	$2.27 \cdot 10^3$	$2.45 \cdot 10^4$	$4.86 \cdot 10^5$	$1.44 \cdot 10^7$	$5.25 \cdot 10^8$	$1.69 \cdot 10^{10}$	$6.30 \cdot 10^{11}$	$2.99 \cdot 10^{13}$
$1 \cdot 10^{-12}$	266.57	$2.27 \cdot 10^3$	$2.45 \cdot 10^4$	$4.86 \cdot 10^5$	$1.44 \cdot 10^7$	$5.25 \cdot 10^8$	$1.69 \cdot 10^{10}$	$6.19 \cdot 10^{11}$	$1.93 \cdot 10^{13}$
$1 \cdot 10^{-11}$	266.57	$2.27 \cdot 10^3$	$2.45 \cdot 10^4$	$4.86 \cdot 10^5$	$1.44 \cdot 10^7$	$5.25 \cdot 10^8$	$1.70 \cdot 10^{10}$	$5.26 \cdot 10^{11}$	$6.28 \cdot 10^{12}$
$1 \cdot 10^{-10}$	266.57	$2.27 \cdot 10^3$	$2.45 \cdot 10^4$	$4.86 \cdot 10^5$	$1.44 \cdot 10^7$	$5.26 \cdot 10^8$	$1.86 \cdot 10^{10}$	$2.02 \cdot 10^{11}$	$1.37 \cdot 10^{12}$
$1 \cdot 10^{-9}$	266.57	$2.27 \cdot 10^3$	$2.45 \cdot 10^4$	$4.86 \cdot 10^5$	$1.44 \cdot 10^7$	$5.34 \cdot 10^8$	$1.29 \cdot 10^{11}$	$5.43 \cdot 10^{11}$	$7.49 \cdot 10^{10}$
$1 \cdot 10^{-8}$	266.57	$2.27 \cdot 10^3$	$2.45 \cdot 10^4$	$4.87 \cdot 10^5$	$1.41 \cdot 10^7$	$6.16 \cdot 10^8$	$5.48 \cdot 10^9$	$8.38 \cdot 10^9$	$3.11 \cdot 10^{10}$
$1 \cdot 10^{-7}$	266.57	$2.27 \cdot 10^3$	$2.45 \cdot 10^4$	$4.93 \cdot 10^5$	$1.21 \cdot 10^7$	$5.85 \cdot 10^8$	$4.48 \cdot 10^8$	$5.82 \cdot 10^8$	$3.83 \cdot 10^9$
$1 \cdot 10^{-6}$	266.54	$2.27 \cdot 10^3$	$2.42 \cdot 10^4$	$5.61 \cdot 10^5$	$4.65 \cdot 10^6$	$7.61 \cdot 10^7$	$6.08 \cdot 10^8$	$8.14 \cdot 10^8$	$1.18 \cdot 10^{10}$
$1 \cdot 10^{-5}$	266.32	$2.30 \cdot 10^3$	$2.17 \cdot 10^4$	$2.15 \cdot 10^6$	$2.39 \cdot 10^6$	$7.03 \cdot 10^6$	$2.28 \cdot 10^7$	$3.24 \cdot 10^7$	$8.87 \cdot 10^7$
$1 \cdot 10^{-4}$	264.09	$2.60 \cdot 10^3$	$1.07 \cdot 10^4$	$1.98 \cdot 10^5$	$1.81 \cdot 10^5$	$7.60 \cdot 10^5$	$3.36 \cdot 10^7$	$3.80 \cdot 10^6$	$5.66 \cdot 10^6$
$1 \cdot 10^{-3}$	243.72	$8.39 \cdot 10^3$	$2.81 \cdot 10^3$	$1.70 \cdot 10^4$	$2.30 \cdot 10^4$	$7.12 \cdot 10^4$	$9.33 \cdot 10^4$	$8.75 \cdot 10^4$	$1.20 \cdot 10^5$

4. NUMERICAL RESULTS AND DISCUSSION

In this section, we explore two examples focusing on inverse Stefan problems in one spatial dimension, where the coefficients of the heat equation are set as $a = 1$, and those in the boundary conditions are $\lambda = 1$, $L = 1$, $\gamma = 1$ and $T = 1$.

To quantify the deviation of the numerical solution from the exact solution, we introduce the root mean square relative error, denoted as Δu for the heat distribution and ΔP for the heat flux:

$$\Delta u = \left[\frac{\int_0^T \int_0^{s(t)} (u(x,t) - u_N(x,t))^2 dx dt}{\int_0^T \int_0^{s(t)} (u(x,t))^2 dx dt} \right]^{1/2}, \quad \Delta P = \left[\frac{\int_0^T \left(-\lambda \frac{\partial u_N(0,t)}{\partial x} - P(t) \right)^2 dt}{\int_0^T (P(t))^2 dt} \right]^{1/2}.$$

Here, $u(x,t)$ and $P(t)$ represent the exact heat temperature and heat flux, while $u_N(x,t)$ and $\frac{\partial u_N(0,t)}{\partial x}$ denote the reconstructed heat temperature and heat flux.

To assess the solution's sensitivity to various noise levels in the measured boundary data, we introduce random noise to the original data. For this purpose, we employ a procedure to generate a set of random real-valued data, which we subsequently add to the exact Neumann data (7), how it was done in [16] as follows:

$$(11) \quad u_x^\epsilon(s(t), t) = L\gamma s'(t) + M(0, \sigma^2)$$

In this equation, $M(0, \sigma^2)$ represents a normal distribution with a mean of zero and a standard deviation of $\sigma = \epsilon \cdot |u_x(s(t), t)| = \epsilon$, where ϵ denotes the relative (percentage) noise level.

TABLE 3. The values ΔP of the relative error depending on the parameters N and β for different noise levels ϵ , Example 4.1.

β	$N = 6$				$N = 8$			
	$C(\mathbf{A}_N, \beta)$	$\Delta P_{\epsilon=1\%}$	$\Delta P_{\epsilon=3\%}$	$\Delta P_{\epsilon=5\%}$	$C(\mathbf{A}_N, \beta)$	$\Delta P_{\epsilon=1\%}$	$\Delta P_{\epsilon=3\%}$	$\Delta P_{\epsilon=5\%}$
0	$2.27 \cdot 10^3$	$1.19 \cdot 10^{-3}$	$7.63 \cdot 10^{-4}$	$1.38 \cdot 10^{-3}$	$2.45 \cdot 10^4$	$6.13 \cdot 10^{-4}$	$4.14 \cdot 10^{-4}$	$5.67 \cdot 10^{-4}$
$1 \cdot 10^{-7}$	$2.27 \cdot 10^3$	$2.07 \cdot 10^{-3}$	$1.45 \cdot 10^{-3}$	$2.23 \cdot 10^{-3}$	$2.45 \cdot 10^4$	$1.44 \cdot 10^{-3}$	$1.90 \cdot 10^{-3}$	$1.67 \cdot 10^{-3}$
$1 \cdot 10^{-6}$	$2.27 \cdot 10^3$	$5.00 \cdot 10^{-3}$	$4.44 \cdot 10^{-3}$	$5.05 \cdot 10^{-3}$	$2.42 \cdot 10^4$	$4.45 \cdot 10^{-3}$	$4.89 \cdot 10^{-3}$	$4.73 \cdot 10^{-3}$
$1 \cdot 10^{-5}$	$2.30 \cdot 10^3$	0.01	0.01	0.01	$2.17 \cdot 10^4$	0.01	0.01	0.01
$1 \cdot 10^{-4}$	$2.60 \cdot 10^3$	0.03	0.03	0.03	$1.07 \cdot 10^4$	0.03	0.03	0.03
$1 \cdot 10^{-3}$	$8.39 \cdot 10^3$	0.10	0.10	0.10	$2.81 \cdot 10^3$	0.10	0.10	0.10

β	$N = 10$				$N = 16$			
	$C(\mathbf{A}_N, \beta)$	$\Delta P_{\epsilon=1\%}$	$\Delta P_{\epsilon=3\%}$	$\Delta P_{\epsilon=5\%}$	$C(\mathbf{A}_N, \beta)$	$\Delta P_{\epsilon=1\%}$	$\Delta P_{\epsilon=3\%}$	$\Delta P_{\epsilon=5\%}$
0	$4.86 \cdot 10^5$	$1.11 \cdot 10^{-3}$	$9.18 \cdot 10^{-4}$	$2.24 \cdot 10^{-3}$	$1.69 \cdot 10^{10}$	$9.84 \cdot 10^{-3}$	0.02	0.02
$1 \cdot 10^{-7}$	$4.93 \cdot 10^5$	$1.68 \cdot 10^{-3}$	$4.75 \cdot 10^{-4}$	$1.76 \cdot 10^{-3}$	$4.48 \cdot 10^8$	$1.94 \cdot 10^{-3}$	$2.01 \cdot 10^{-3}$	$2.57 \cdot 10^{-3}$
$1 \cdot 10^{-6}$	$5.61 \cdot 10^5$	$4.21 \cdot 10^{-3}$	$3.33 \cdot 10^{-3}$	$4.01 \cdot 10^{-3}$	$6.08 \cdot 10^8$	$5.13 \cdot 10^{-3}$	$5.18 \cdot 10^{-3}$	$5.44 \cdot 10^{-3}$
$1 \cdot 10^{-5}$	$2.15 \cdot 10^6$	0.01	0.01	0.01	$2.28 \cdot 10^7$	0.01	0.01	0.01
$1 \cdot 10^{-4}$	$1.98 \cdot 10^5$	0.04	0.04	0.04	$3.36 \cdot 10^7$	0.04	0.04	0.04
$1 \cdot 10^{-3}$	$1.70 \cdot 10^4$	0.11	0.11	0.11	$9.33 \cdot 10^4$	0.13	0.13	0.13

4.1. Example 1.

To demonstrate the proposed method, we consider a specific benchmark example for which an analytical solution can be derived (see [14, 32, 16]). The exact solution and the moving boundary are given by:

$$u(x, t) = -1 + \exp\left(1 - \frac{1}{\sqrt{2}} + \frac{t}{2} - \frac{x}{\sqrt{2}}\right), \quad \text{in } 0 < x < s(t), \quad 0 < t \leq 1,$$

$$s(t) = \sqrt{2} - 1 + \frac{t}{\sqrt{2}}.$$

The initial and boundary conditions for the problem are given as follows.

$$f(x) = -1 + \exp\left(1 - \frac{1}{\sqrt{2}} - \frac{x}{\sqrt{2}}\right), \quad s_0 = \sqrt{2} - 1, \quad x \in [0, s(0)],$$

$$P(t) = \frac{-1}{\sqrt{2}} \exp\left(1 - \frac{1}{\sqrt{2}} + \frac{t}{2}\right), \quad u^* = 0, \quad t \in [0, 1].$$

In this section, we reformulate the inverse Stefan problem as discussed in Section 2, where the goal is to find a solution satisfying Eqs. (3)-(8) and recover the Neumann boundary condition (5):

$$(12) \quad \frac{\partial u}{\partial x}(0, t) = \frac{-1}{\sqrt{2}} \exp\left(1 - \frac{1}{\sqrt{2}} + \frac{t}{2}\right), \quad t \in [0, 1].$$

We approximate the solution $u(x, t)$ in the form of Eq. (9), where $v_n(x, t)$ is defined by Eq. (2). The coefficients c_n are determined from the system of equations (10), which is obtained by satisfying the initial condition (4) and boundary conditions (6), (7). This system is solved using the matrix inversion method.

The relative errors for the reconstructed heat flux $P(t)$ for different values of β and N with noise-free data are shown in Table 1. From the table, it can be observed that for small values of N and β , the regularization parameter β has little effect on the recovery results. However, for larger values of $N \geq 10$, regardless of how small β is chosen, the unregularized solution provides better results. In other words, for noise-free data, setting $\beta = 0$ may yield the best results.

Since the matrix \mathbf{A} can be computed independently before any measurements, the condition numbers $C(\mathbf{A}_N, \alpha)$ can be determined for different values of N and β . This enables the identification of the most suitable combinations of N and β . Table 2 shows the condition number

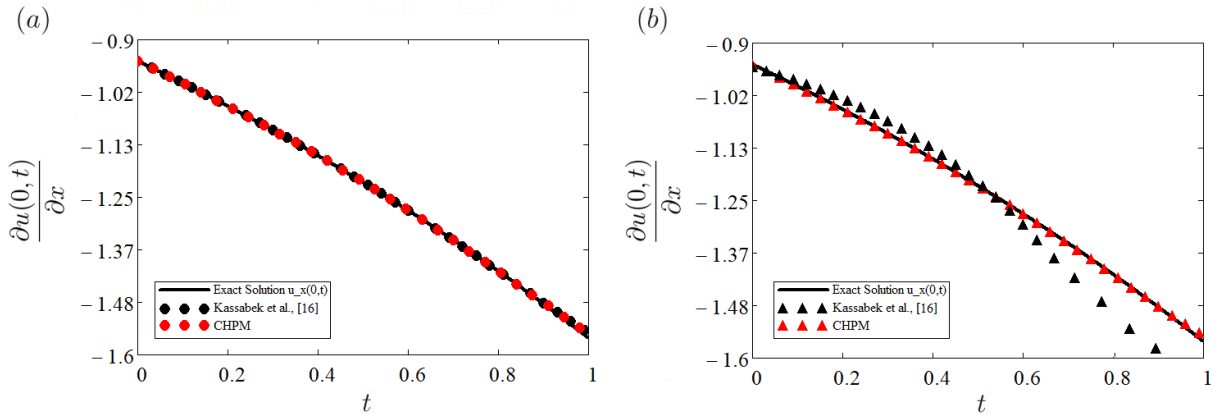


FIGURE 2. For Example 4.1 of the inverse Stefan problem, graphs of the reconstructed heat flux $u_x(0, t)$ for different noise levels: (a) $\epsilon = 1\%$, (b) $\epsilon = 5\%$ obtained by CHPM with $N = 12$ and by Kassabek et al. [16] using HPM with $N = 12$.

$C(\mathbf{A}_N, \beta)$ for various values of β . The results indicate that the condition number is highly sensitive to the choice of N . As seen in the table, $C(\mathbf{A}_N, \beta)$ increases significantly as N increases and decreases with larger β , revealing a trade-off between stability and accuracy. Stability can be improved by decreasing N and selecting a sufficiently large β , but this comes at the cost of accuracy in approximating the function $P(t)$.

To assess the sensitivity of the proposed method, we introduce random noise to the boundary data $s'(t)$ and to $u_x(s(t), t)$, as outlined in Eq. (11). The reconstructed heat flux $P(t)$ for noise levels of $\epsilon = 1\%$, $\epsilon = 3\%$, and $\epsilon = 5\%$ is shown in Figs. 1 and 2, with $N = 12$. Fig. 1(a) and 1(b) illustrate the CHPM approximations of the Neumann boundary condition (12) and the corresponding absolute error for these noise levels, using polynomials of degree $N = 12$. The numerical results in Fig. 2 align well with those presented by Kassabek et al. [16], who used the HPM method with $N = 12$. It is important to note that the results presented in Figs. 1 and 2 were obtained without applying regularization, whereas in [16], Tikhonov regularization was used to obtain the numerical results.

Table 3 examines various combinations of (N, β) with noisy data and identifies the optimal ones. The results show that higher noise levels require a smaller regularization parameter and a reduced cut-off number N . The first test problem considers the time interval $[0, 1]$. To evaluate the method's effectiveness for long-term processes, we also consider different values of T . The numerical results, summarized in Table 4, indicate that increasing T affects the solution's accuracy.

The numerical results for the first test problem differ from the previous results presented in [16], as shown in Table 5. This table presents the results obtained using two methods: the collocation heat polynomials method (CHPM) and the variational heat polynomials method (VHPM). As seen in Table 5, the VHPM method performs better for $N \leq 10$, but its accuracy decreases for larger values of N . In contrast, the results obtained by CHPM remain more stable as N increases. Additionally, the CHPM results are sensitive to the choice of discretization for both the spatial domain $[0, s(0)]$ and the time domain $[0, T]$ when divided into finite intervals.

By integrating conditions (4), (6), and (7) and substituting the approximate solution in the form of (9) on the left-hand side, a system of equations is formed. Since there are two boundary conditions on $s(t)$, namely the Dirichlet condition (6) and the Stefan condition (7), various discretization strategies can be applied to the time domain $[0, T]$.

An interesting observation regarding the choice of discretization is that the best results are obtained when the spatial interval $[0, s(0)]$ is divided into two subintervals or not divided at all. For example, if we choose to divide $[0, s(0)]$ into two equal subintervals, integrating the initial

TABLE 4. Values $P(t)$ of the relative error for different time intervals $[0, T]$ with zero noise, Example 4.1.

$T \setminus N$	4	6	8	10	12	14	16	18	20
1	$1.84 \cdot 10^{-2}$	$1.90 \cdot 10^{-3}$	$1.08 \cdot 10^{-4}$	$4.80 \cdot 10^{-6}$	$1.72 \cdot 10^{-7}$	$5.06 \cdot 10^{-9}$	$6.57 \cdot 10^{-11}$	$1.67 \cdot 10^{-11}$	$2.05 \cdot 10^{-11}$
2	0.11	$1.30 \cdot 10^{-2}$	$1.32 \cdot 10^{-3}$	$9.48 \cdot 10^{-5}$	$4.93 \cdot 10^{-6}$	$4.30 \cdot 10^{-7}$	$5.06 \cdot 10^{-8}$	$1.59 \cdot 10^{-9}$	$1.91 \cdot 10^{-10}$
3	0.85	$3.66 \cdot 10^{-2}$	$4.51 \cdot 10^{-3}$	$5.23 \cdot 10^{-4}$	$1.80 \cdot 10^{-4}$	$4.30 \cdot 10^{-5}$	$6.32 \cdot 10^{-7}$	$8.69 \cdot 10^{-7}$	$3.29 \cdot 10^{-9}$
4	1.90	$6.74 \cdot 10^{-2}$	$1.02 \cdot 10^{-2}$	$8.17 \cdot 10^{-3}$	$4.39 \cdot 10^{-3}$	$2.28 \cdot 10^{-3}$	$1.62 \cdot 10^{-5}$	$3.89 \cdot 10^{-5}$	$2.42 \cdot 10^{-7}$
5	1.04	$9.11 \cdot 10^{-2}$	$7.17 \cdot 10^{-2}$	0.13	$8.77 \cdot 10^{-2}$	$6.56 \cdot 10^{-3}$	$6.37 \cdot 10^{-4}$	$9.94 \cdot 10^{-5}$	$1.34 \cdot 10^{-5}$

TABLE 5. The values of relative error for heat distribution $u(x, t)$ and heat flux $P(t)$ obtained by CHPM and VHPM with zero noise, Example 4.1.

N	Collocation method		Variational method	
	Δu	ΔP	Δu	ΔP
4	0.014	0.018	$4.250 \cdot 10^{-3}$	$8.195 \cdot 10^{-3}$
6	$5.064 \cdot 10^{-3}$	$3.064 \cdot 10^{-4}$	$2.846 \cdot 10^{-4}$	$6.801 \cdot 10^{-4}$
8	$3.013 \cdot 10^{-4}$	$1.086 \cdot 10^{-4}$	$1.458 \cdot 10^{-5}$	$4.243 \cdot 10^{-5}$
10	$1.266 \cdot 10^{-6}$	$1.459 \cdot 10^{-5}$	$5.824 \cdot 10^{-7}$	$2.009 \cdot 10^{-6}$
12	$3.69 \cdot 10^{-8}$	$3.639 \cdot 10^{-7}$	$1.187 \cdot 10^{-7}$	$7.923 \cdot 10^{-8}$
14	$9.088 \cdot 10^{-10}$	$5.06 \cdot 10^{-9}$	$2.504 \cdot 10^{-7}$	$1.190 \cdot 10^{-7}$

condition (4) over each subinterval, we obtain two equations. To solve a system of size $N \times N$, the time interval $[0, T]$ for each boundary condition (6) and (7) can either be divided equally, or for condition (6), the number of points used to divide $[0, T]$ must be more than that for the Stefan condition (7).

The results shown in Figs. 1 and 2 were obtained for $N = 12$, where we solved a 13×13 system. In this case, condition (6) was divided into 6 intervals, condition (7) into 5 intervals, and condition (4) into 2 intervals. By integrating these conditions over their respective intervals, we obtain the necessary system of equations.

4.2. Example 2.

As the second example [16], we consider the moving boundary function

$$s(t) = 2a\sqrt{t + t_0},$$

where $t_0 = 0.162558$ and $\alpha = 0.620063$ with the exact solution given by

$$u(x, t) = 1 - \frac{\operatorname{erf}\left(\frac{x}{2\sqrt{t+t_0}}\right)}{\operatorname{erf}(\alpha)}.$$

The initial and boundary conditions considered in the problem are given by

$$f(x) = 1 - \frac{\operatorname{erf}\left(\frac{x}{2\sqrt{t_0}}\right)}{\operatorname{erf}(\alpha)}, \quad s_0 = 2a\sqrt{t_0}, \quad x \in [0, s(0)],$$

$$P(t) = -\frac{1}{\sqrt{\pi(t+t_0)}\operatorname{erf}(\alpha)}, \quad u^* = 0, \quad t \in [0, 1].$$

In the second test example, the heat flux to be recovered follows the form:

$$\frac{\partial u}{\partial x}(0, t) = -\frac{1}{\sqrt{\pi(t+t_0)}\operatorname{erf}(\alpha)}, \quad t \in [0, 1].$$

Table 6 presents the relative errors for the reconstructed heat flux $P(t)$ with various values of β and N under noise-free conditions. As in Example 4.1, for smaller values of N and β , the regularization parameter β has minimal impact on the recovery results. However, for larger

TABLE 6. The values ΔP of the relative error depending on the parameters N and β with zero noise, Example 4.2.

$\beta \setminus N$	4	6	8	10	12	14	16	18	20
0	0.042	0.042	0.024	0.028	0.03	0.111	0.361	0.148	0.147
$1 \cdot 10^{-13}$	0.098	0.042	0.024	0.029	0.022	0.09	0.105	0.099	0.09
$1 \cdot 10^{-12}$	0.098	0.042	0.024	0.032	0.013	0.125	0.174	0.17	0.189
$1 \cdot 10^{-11}$	0.098	0.042	0.024	0.034	0.042	0.303	0.335	0.32	0.32
$1 \cdot 10^{-10}$	0.098	0.042	0.024	0.024	0.024	0.16	0.161	0.147	0.137
$1 \cdot 10^{-9}$	0.098	0.042	0.05	0.053	0.09	0.123	0.141	0.162	0.176
$1 \cdot 10^{-8}$	0.098	0.043	0.069	0.079	0.091	0.298	0.3	0.31	0.312
$1 \cdot 10^{-7}$	0.099	0.058	0.069	0.047	0.044	0.143	0.138	0.13	0.124
$1 \cdot 10^{-6}$	0.099	0.131	0.139	0.139	0.135	0.151	0.153	0.174	0.185
$1 \cdot 10^{-5}$	0.101	0.128	0.127	0.122	0.118	0.201	0.202	0.207	0.209
$1 \cdot 10^{-4}$	0.146	0.151	0.135	0.147	0.147	0.104	0.104	0.11	0.114
$1 \cdot 10^{-3}$	0.264	0.29	0.239	0.239	0.236	0.225	0.226	0.226	0.226

TABLE 7. The condition number $C(\mathbf{A}_N, \beta)$ depending on the parameters N and β with zero noise, Example 4.2.

$\beta \setminus N$	4	6	8	10	12	14	16	18	20
0	134.90	$2.30 \cdot 10^3$	$4.26 \cdot 10^4$	$4.90 \cdot 10^5$	$1.97 \cdot 10^7$	$7.57 \cdot 10^8$	$2.53 \cdot 10^{10}$	$2.53 \cdot 10^{12}$	$7.38 \cdot 10^{13}$
$1 \cdot 10^{-13}$	134.90	$2.30 \cdot 10^3$	$4.26 \cdot 10^4$	$4.90 \cdot 10^5$	$1.97 \cdot 10^7$	$7.57 \cdot 10^8$	$2.53 \cdot 10^{10}$	$1.41 \cdot 10^{12}$	$7.86 \cdot 10^{13}$
$1 \cdot 10^{-12}$	134.90	$2.30 \cdot 10^3$	$4.26 \cdot 10^4$	$4.90 \cdot 10^5$	$1.97 \cdot 10^7$	$7.57 \cdot 10^8$	$2.53 \cdot 10^{10}$	$1.38 \cdot 10^{12}$	$2.18 \cdot 10^{14}$
$1 \cdot 10^{-11}$	134.90	$2.30 \cdot 10^3$	$4.26 \cdot 10^4$	$4.90 \cdot 10^5$	$1.97 \cdot 10^7$	$7.57 \cdot 10^8$	$2.56 \cdot 10^{10}$	$1.14 \cdot 10^{12}$	$1.09 \cdot 10^{13}$
$1 \cdot 10^{-10}$	134.90	$2.30 \cdot 10^3$	$4.26 \cdot 10^4$	$4.90 \cdot 10^5$	$1.97 \cdot 10^7$	$7.55 \cdot 10^8$	$2.88 \cdot 10^{10}$	$3.88 \cdot 10^{11}$	$2.90 \cdot 10^{12}$
$1 \cdot 10^{-9}$	134.90	$2.30 \cdot 10^3$	$4.26 \cdot 10^4$	$4.90 \cdot 10^5$	$1.97 \cdot 10^7$	$7.39 \cdot 10^8$	$9.67 \cdot 10^{10}$	$7.98 \cdot 10^{10}$	$1.92 \cdot 10^{12}$
$1 \cdot 10^{-8}$	134.90	$2.30 \cdot 10^3$	$4.26 \cdot 10^4$	$4.90 \cdot 10^5$	$1.98 \cdot 10^7$	$6.06 \cdot 10^8$	$1.62 \cdot 10^{10}$	$1.15 \cdot 10^{10}$	$1.16 \cdot 10^{11}$
$1 \cdot 10^{-7}$	134.90	$2.30 \cdot 10^3$	$4.26 \cdot 10^4$	$4.89 \cdot 10^5$	$2.17 \cdot 10^7$	$1.91 \cdot 10^8$	$6.39 \cdot 10^8$	$2.98 \cdot 10^9$	$5.27 \cdot 10^{10}$
$1 \cdot 10^{-6}$	134.90	$2.30 \cdot 10^3$	$4.28 \cdot 10^4$	$4.77 \cdot 10^5$	$5.50 \cdot 10^7$	$5.25 \cdot 10^7$	$1.66 \cdot 10^7$	$2.42 \cdot 10^9$	$4.00 \cdot 10^9$
$1 \cdot 10^{-5}$	134.92	$2.30 \cdot 10^3$	$4.45 \cdot 10^4$	$3.76 \cdot 10^5$	$6.42 \cdot 10^6$	$6.57 \cdot 10^6$	$9.04 \cdot 10^6$	$4.41 \cdot 10^7$	$7.64 \cdot 10^8$
$1 \cdot 10^{-4}$	135.13	$2.25 \cdot 10^3$	$7.28 \cdot 10^4$	$2.07 \cdot 10^5$	$5.58 \cdot 10^5$	$4.73 \cdot 10^5$	$5.85 \cdot 10^5$	$3.39 \cdot 10^6$	$3.38 \cdot 10^6$
$1 \cdot 10^{-3}$	137.35	$1.87 \cdot 10^3$	$2.69 \cdot 10^4$	$9.07 \cdot 10^4$	$4.13 \cdot 10^4$	$5.29 \cdot 10^4$	$1.18 \cdot 10^5$	$1.17 \cdot 10^5$	$1.12 \cdot 10^5$

values of $N \geq 12$, smaller values of β perform better than the unregularized solution, which contrasts with the results from the previous test problems.

Table 7 presents the condition number $C(\mathbf{A}_N, \beta)$ for different values of β . The results demonstrate that, similar to Example 4.1, the condition number is highly sensitive to the selection of N . As shown in Table 7, $C(\mathbf{A}_N, \beta)$ increases significantly with larger N and decreases with higher values of β .

The reconstructed heat flux $P(t)$ and the corresponding absolute errors for noise levels of $\epsilon = 1\%$, $\epsilon = 3\%$, and $\epsilon = 5\%$ are shown in Figs. 3, 4, and 5 for $N = 10$. To compare our numerical solution with the previously obtained results by [16] (HPM for $N = 10$), we consider the time interval $[0, 0.5]$, as illustrated in Fig. 5. It is important to note that no regularization was applied to the results presented in any of the figures.

By examining various combinations of (N, β) with noisy data, similar to Example 4.1, we observe that higher noise levels require a smaller regularization parameter and a lower cut-off number N , as shown in Table 8. Additionally, Table 9 demonstrates that increasing the time interval T impacts the accuracy of the solution.

In the case of the second test problem, the CHPM method yielded better results than the VHPM method for all investigated orders of N . The numerical solution results are presented in Table 10. As in Example 4.1, we employed a non-equal partitioning of the interval $(0, s(0))$ for conditions (6) and (7). The results shown in Figures 3, 4, and 5 were obtained with $N = 10$,

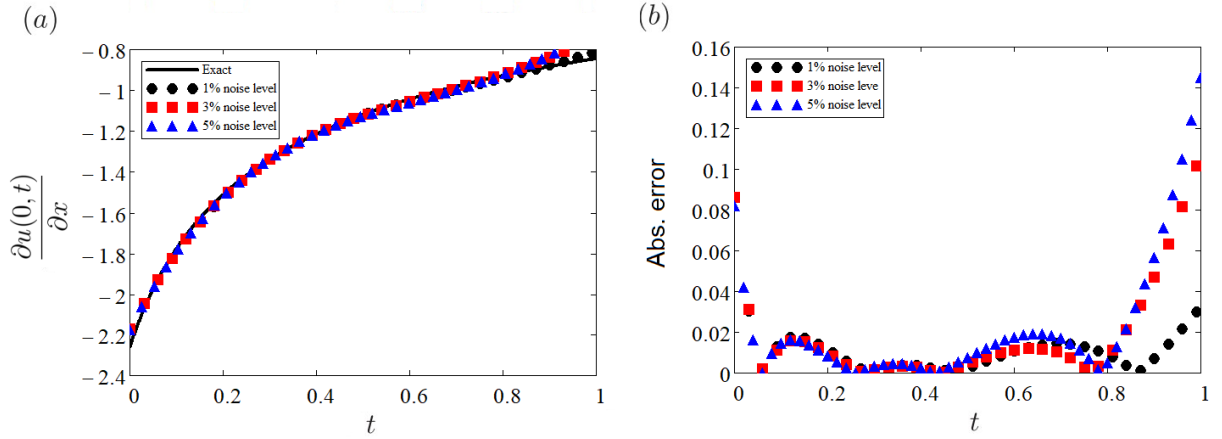


FIGURE 3. For Example 4.2 of the inverse Stefan problem (a) depicts the comparison between the exact and approximate solutions of $u_x(0, t)$, (b) illustrates the absolute error between the exact solution and $u_x(0, t)$ for different noise levels for $N = 10$.

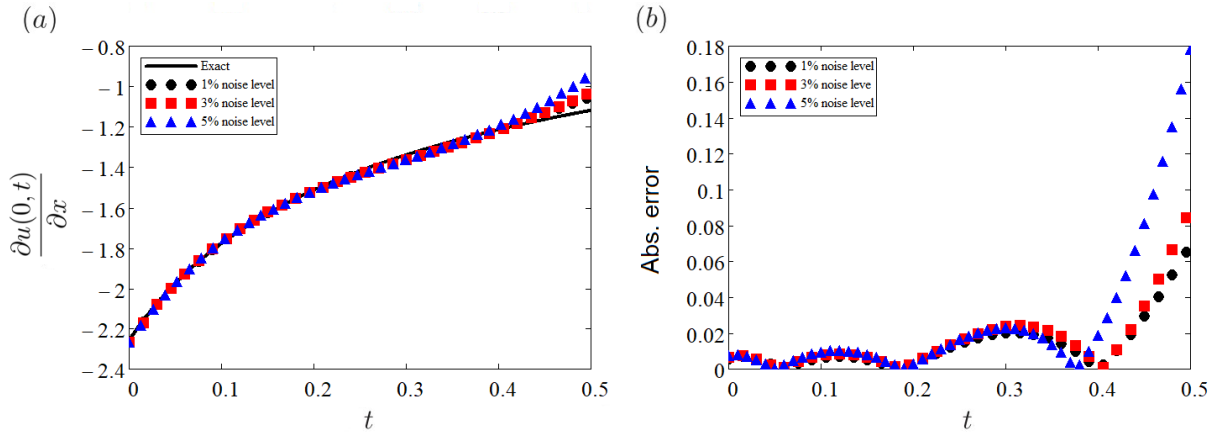


FIGURE 4. For Example 4.2 of the inverse Stefan problem (a) depicts the comparison between the exact and approximate solutions of $u_x(0, t)$, (b) illustrates the absolute error between the exact solution and $u_x(0, t)$ for different noise levels for $N = 10$.

where an 11×11 system was solved. Specifically, condition (6) was divided into six intervals, condition (7) into four intervals, and condition (4) into one interval.

Overall, the numerical results in this section demonstrate that CHPM approximations offer both accuracy and stability, comparing favorably to exact solutions and yielding better outcomes than those in [16]. While increasing the number of heat polynomials initially improves the results, using too many can result in ill-conditioned problems. Nevertheless, with greater computational power, better outcomes may be achieved for higher values of N . From the two numerical test cases, we observe that an error of less than 5% can be achieved by using $N = 4$ by solving a 5×5 linear system of equations.

To provide a theoretical foundation for our method, we refer to the works of [16, 36, 43], which are summarized in the following theorem:

TABLE 8. The values ΔP of the relative error depending on the parameters N and β for different noise levels ϵ , Example 4.2.

β	$N = 6$				$N = 8$			
	$C(\mathbf{A}_N, \beta)$	$\Delta P_{\epsilon=1\%}$	$\Delta P_{\epsilon=3\%}$	$\Delta P_{\epsilon=5\%}$	$C(\mathbf{A}_N, \beta)$	$\Delta P_{\epsilon=1\%}$	$\Delta P_{\epsilon=3\%}$	$\Delta P_{\epsilon=5\%}$
0	$2.308 \cdot 10^3$	0.041	0.0416	0.0428	$4.262 \cdot 10^4$	0.0228	0.0232	0.031
$1 \cdot 10^{-7}$	$2.307 \cdot 10^3$	0.0561	0.0572	0.0596	$4.264 \cdot 10^4$	0.0672	0.0685	0.0649
$1 \cdot 10^{-6}$	$2.307 \cdot 10^3$	0.1294	0.1305	0.1333	$4.28 \cdot 10^4$	0.1366	0.1269	0.1366
$1 \cdot 10^{-5}$	$2.302 \cdot 10^3$	0.1271	0.1276	0.1295	$4.453 \cdot 10^4$	0.126	0.127	0.126
$1 \cdot 10^{-4}$	$2.251 \cdot 10^3$	0.1517	0.1516	0.1503	$7.285 \cdot 10^4$	0.1352	0.1353	0.1358
$1 \cdot 10^{-3}$	$1.871 \cdot 10^3$	0.2899	0.29	0.2892	$2.692 \cdot 10^4$	0.238	0.239	0.2388

β	$N = 10$				$N = 16$			
	$C(\mathbf{A}_N, \beta)$	$\Delta P_{\epsilon=1\%}$	$\Delta P_{\epsilon=3\%}$	$\Delta P_{\epsilon=5\%}$	$C(\mathbf{A}_N, \beta)$	$\Delta P_{\epsilon=1\%}$	$\Delta P_{\epsilon=3\%}$	$\Delta P_{\epsilon=5\%}$
0	$4.908 \cdot 10^5$	0.0174	0.0246	0.0254	$2.536 \cdot 10^{10}$	0.0543	0.1208	0.1253
$1 \cdot 10^{-7}$	$4.894 \cdot 10^5$	0.0465	0.0468	0.0455	$6.396 \cdot 10^8$	0.139	0.1384	0.1389
$1 \cdot 10^{-6}$	$4.771 \cdot 10^5$	0.1391	0.1397	0.138	$1.668 \cdot 10^7$	0.1523	0.1518	0.1518
$1 \cdot 10^{-5}$	$3.767 \cdot 10^5$	0.1214	0.122	0.1211	$9.041 \cdot 10^6$	0.2019	0.2018	0.2023
$1 \cdot 10^{-4}$	$2.075 \cdot 10^5$	0.1471	0.1467	0.1469	$5.856 \cdot 10^5$	0.1041	0.1042	0.1038
$1 \cdot 10^{-3}$	$9.077 \cdot 10^4$	0.2389	0.2387	0.2387	$1.183 \cdot 10^5$	0.2255	0.2257	0.2253

TABLE 9. Values $P(t)$ of the relative error for different time intervals $[0, T]$ with zero noise, Example 4.2.

$T \setminus N$	4	6	8	10	12	14	16	18	20
1	0.1	0.04	0.02	0.03	0.03	0.11	0.36	0.15	0.15
2	0.43	0.54	0.55	0.69	7.45	96.25	621.04	$1.21 \cdot 10^3$	$3.58 \cdot 10^3$
3	1.05	2.4	4.46	2.93	114.11	$1.80 \cdot 10^3$	$1.97 \cdot 10^4$	$6.58 \cdot 10^4$	$3.24 \cdot 10^5$
4	1.84	5.97	16.11	28.32	700.17	$1.28 \cdot 10^4$	$2 \cdot 10^5$	$9.46 \cdot 10^5$	$6.53 \cdot 10^6$
5	2.76	11.57	40.86	114.19	$2.72 \cdot 10^3$	$5.67 \cdot 10^4$	$1.16 \cdot 10^6$	$7.07 \cdot 10^6$	$6.28 \cdot 10^7$

4.1. **Theorem.** Let $u(x, t)$ be the unique solution of the problem (3)-(8) and let

$$u_N(x, t) = \sum_{n=0}^N a_n^{(N)} v_n(x, t)$$

be a sequence of polynomials such that:

- (a) $\lim_{N \rightarrow \infty} \|Su_N - r\| = 0$
- (b) $\left| a_n^{(N)} \right| \leq C \left(\frac{e}{2nt_0} \right)^{n/2}$ for all n and for $N = 0, 1, \dots$, where $C > 0$ is a constant and $t_0 > T$.

Then:

- (1) $\lim_{N \rightarrow \infty} a_n^{(N)} = b_n$
- (2) $\lim_{N \rightarrow \infty} \left\| \frac{\partial^k}{\partial x^k} u_N(x, t) - \frac{\partial^k}{\partial x^k} u(x, t) \right\|_D = 0$ for all $k = 0, 1, \dots$,
 where $u(x, t) = \sum_{n=0}^{\infty} b_n v_n(x, t)$, S is the trace operator defined by $Su = (u(s(\cdot), \cdot), u_x(s(\cdot), \cdot), u(\cdot, 0))$, and the product norm $r = (g(\cdot), \dot{s}(\cdot), f(\cdot))$, with " ." representing the independent variables t or x .

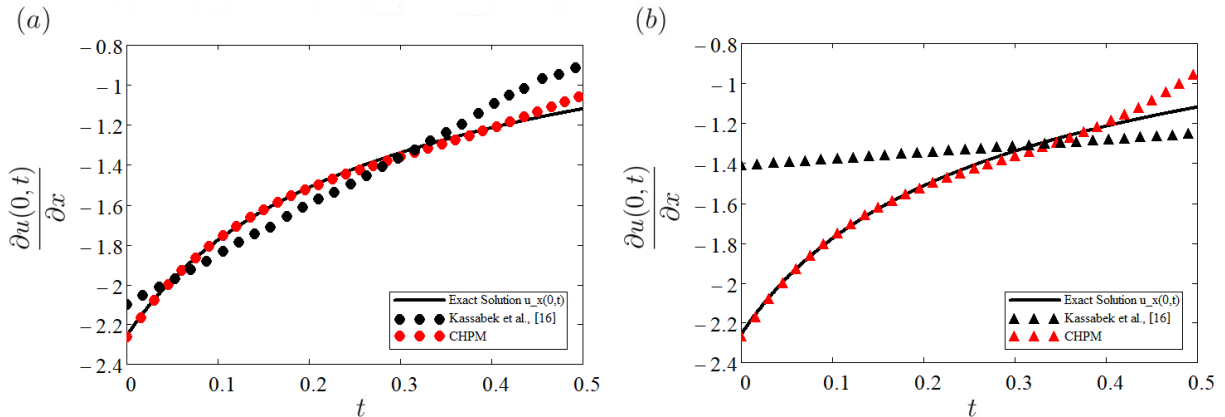


FIGURE 5. For Example 4.2 of the inverse Stefan problem, graphs of the reconstructed heat flux $u_x(0, t)$ for different noise levels: (a) $\epsilon = 1\%$, (b) $\epsilon = 5\%$ obtained by CHPM with $N = 10$ and by Kassabek et al. [16] using HPM with $N = 10$.

TABLE 10. The values of relative error for heat distribution $u(x, t)$ and heat flux $P(t)$ obtained by CHPM and VHPM with zero noise, Example 4.2.

N	Collocation method		Variational method	
	Δu	ΔP	Δu	ΔP
4	0.043	0.042	0.201	0.419
6	0.017	0.042	0.128	0.368
8	$9.599 \cdot 10^{-3}$	0.024	0.049	0.192
10	$6.862 \cdot 10^{-3}$	0.028	0.013	0.033
12	$8.281 \cdot 10^{-3}$	0.03	0.039	0.170
14	0.017	0.111	0.043	0.227

5. CONCLUSION

Up until now, the heat polynomials method has been applied to solve both one- and two-phase inverse Stefan problems, where the solution in the form (9) satisfies the initial and boundary conditions. The unknown coefficients c_n ($n = 1, 2, \dots, N$) are determined from the variational principle, similar to the Trefftz method. In this paper, we applied the collocation method using heat polynomials as basis functions to estimate the temperature distribution and heat flux at the boundary $x = 0$ for inverse one-phase Stefan problems.

The two numerical examples presented in this paper demonstrate a notably high level of accuracy and stability compared to the exact solution. As shown in Tables 1 and 6, an error of less than 5% can be achieved using $N = 4$ by solving a 5×5 system of equations. Moreover, Table 6 shows that in the second test problem, the accuracy of the solution improves significantly by increasing the order N to 12. Similarly, in the first problem, accuracy improves as N increases to 18. Based on these results, we conclude that good results can be obtained by choosing values of N up to 12. At this level, regularization is not needed, as the results indicate that its impact is minimal or does not improve the solution at all.

The numerical results obtained using CHPM differ significantly from those obtained earlier with VHPM, as shown in [16]. The VHPM method performs better for $N \leq 10$, but its accuracy declines for larger values of N , as seen in Table 5. In contrast, the results obtained using CHPM remain more stable as N increases.

As demonstrated in Theorem 4.1, better results can be achieved by increasing the order of N ; however, this increase also raises the condition number of the system, potentially leading to numerical instability. To address this, future research can focus on obtaining more stable solutions in the form of linear combinations of heat polynomials by implementing several strategies.

First, regularization techniques, such as Tikhonov regularization, can help mitigate the ill-conditioning inherent in inverse Stefan problems by penalizing large coefficient values. Additionally, selecting the optimal order N of the heat polynomials is crucial for balancing accuracy and stability, thereby avoiding overfitting and instability.

Moreover, applying scaling techniques can prevent numerical instabilities caused by large variations in polynomial magnitudes. Preconditioning the system of equations, as outlined in [27], can effectively reduce the condition number and further improve stability. Finally, post-conditioning methods, which adjust the coefficients after solving the system, can refine the solution, enhancing accuracy and reducing residual errors [26].

The mathematical simplicity of CHPM makes it well-suited for both nonlinear inverse Stefan problems and direct Stefan problems. Future work will focus on extending the CHPM to address source inverse Stefan-type problems.

6. ACKNOWLEDGEMENTS

The authors sincerely thank the reviewers for their constructive comments and suggestions, which have significantly improved the quality of this paper.

Special thanks go to Prof. Balgaisha Mukanova for her valuable insights and contributions, which greatly helped in refining the numerical aspects of this manuscript.

REFERENCES

- [1] D. D. Ang, A. Pham Ngoc Dinh, D. Trinh, *An inverse Stefan problem: identification of boundary value*, J. Comput. Appl. Math. 66 pp. 75-84, (1996).
- [2] P. Appell, *Sur l'équation $\partial^2 z/\partial x^2 - \partial z/\partial y = 0$ et la théorie de la chaleur*, Journal de Mathématiques Pures et Appliquées, 8, pp. 187-216, (1892).
- [3] Chifaa Ghanmi, Saloua Mani Aouadi & Faouzi Triki (2022), *Identification of a boundary influx condition in a one-phase Stefan problem*, Applicable Analysis, 101:18, 6573-6595.
- [4] S. Futakiewicz L. Hozejowski, *Heat polynomials method in solving the direct and inverse heat conduction problems in a cylindrical system of coordinates*, Transactions on Engineering Sciences vol. 20, 1998 WIT Press, www.witpress.com, ISSN 1743-3533.
- [5] N. L. Goldman, *Inverse Stefan problem*, Kluwer, Dordrecht, (1997).
- [6] K. Grysa, *Heat polynomials and their applications*, A Archives of Thermodynamics, vol. 24 (2003) No. 2, pp. 107-124.
- [7] MJ Cialkowski, K. Grysa, *Trefftz method in solving the inverse problems*, J Inv Ill-Posed Probl, vol.18(6), pp.595-616, (2010).
- [8] K. Grysa, A. Maciag, A. Pawinska, *Solving nonlinear direct and inverse problems of stationary heat transfer by using Trefftz functions*, Int J Heat Mass Transf, vol. 55, pp. 7336-40., (2012).
- [9] K. Grysa, B. Maciejewska, *Trefftz functions for non-stationary problems*, J Theor Appl Mech; vol. 51(2), pp. 251-64, (2013).
- [10] R. Grzymkowski and D. Slota, *One-phase inverse Stefan problems solved by Adomain decomposition method*, Comput. Math. Appl., vol. 51, pp. 33-40, (2006).
- [11] S. C. Gupta, *The classical Stefan problem*. Basic Concepts, Modeling and Analysis, Elsevier, Amsterdam, (2003).
- [12] D.T. Haimo, *Series Representation of Generalized Temperature Functions*, SIAM Journal of Applied Mathematics, v. 15, N. 2, pp. 359-367, (1967).
- [13] L. Hozejowski, *Heat polynomials and their application in direct and inverse problems of heat conduction*, 1999, PHD Theses, Politechnika Świętokrzyska [in Polish]
- [14] B. T. Johansson, D. Lesnic and T. Reeve, *A method of fundamental solutions for the one-dimensional inverse Stefan problem*. Applied Mathematical Modelling, 35, pp. 4367-4378, (2011).
- [15] B. T. Johansson, D. Lesnic and T. Reeve, *A meshless method for an inverse two-phase one-dimensional linear Stefan problem*, Inverse Prob. Sci. Eng. 21 (1), pp. 17-33, (2013).
- [16] S. A. Kassabek, S. N. Kharin, D. Suragan, *A heat polynomials method for inverse cylindrical one-phase Stefan problems*, Inverse Problems in Science and Engineering, vol 29, pp. 3423-3450, (2021).
- [17] S. A. Kassabek, D. Suragan, *Numerical approximation of the one-dimensional inverse Cauchy-Stefan problem using heat polynomials methods*, Computational and Applied Mathematics, 41(4), doi.org/10.1007/s40314-022-01896-1, (2022).
- [18] S. A. Kassabek, D. Suragan, *Two-phase inverse Stefan problems solved by heat polynomials method*, Journal of Computational and Applied Mathematics, 421, (2023), 114854.
- [19] S. A. Kassabek, D. Suragan, *A heat polynomials method for the two-phase inverse Stefan problem*, Computational and Applied Mathematics (2023) 42:129

- [20] S. A. Kassabek, T. A. Nauryz, Amankeldy Toleukhanov, *Analytical solution of Stefan type problems*, (2024), Journal of Inverse and Ill-Posed Problems, doi: 10.1515/jiip-2021-0077.
- [21] D. Ślota, *Homotopy perturbation method for solving the two-phase inverse Stefan problem*, Numerical Heat Transfer, Part A 59, pp. 775-768, (2011).
- [22] M. Nawaz Khan, I. Ahmad, H. Ahmad, *A Radial Basis Function Collocation Method for Space-dependent Inverse Heat Problems*, J. Appl. Comput. Mech. 6(SI) (2020) 1187-1199.
- [23] S. N. Kharin, M. M. Sarsengeldin, and H. Nouri, *Analytical solution of two-phase spherical Stefan problem by heat polynomials and integral error functions*, AIP Conference Proceedings 1759, 020031 (2016).
- [24] S. N. Kharin, *Mathematical models of phenomena in electrical contacts*. A.P. Ershov Institute of Informatics System The Russian Academy of Sciences, Siberian Branch, Novosibirsk, (2017).
- [25] S. N. Kharin, *Special functions and heat polynomials for the solution of free boundary problems*, AIP Conference Proceedings 1997, 020047; (2020).
- [26] C.-S. Liu, *The method of fundamental solutions for solving the backward heat conduction problem with conditioning by a new post-conditioner*, Numer. Heat Transfer, B: Fundam., vol. 60, pp. 57-72, (2011).
- [27] C.-S. Liu, *A two-side equilibration method to reduce the condition number of an ill-posed linear system*, Comput. Model. Eng. Sci., vol. 91, pp. 17-42, (2013).
- [28] C.S. Liu, *A multiple scale direction polynomial Trefftz method for solving the BHCP in high-dimensional arbitrary simply-connected domains*, Int. J. Heat Mass Transfer 92 (2016) 970-978.
- [29] B. Maciejewska, M. Piasecka, *An application of the non-continuous Trefftz method to the determination of heat transfer coefficient for flow boiling in a minichannel*. Heat Mass Transf. 2017, 53, 1211-1224.
- [30] B. Maciejewska, M. Piasecka, *Trefftz function-based thermal solution of inverse problem in unsteady-state flow boiling heat transfer in a minichannel*. Int. J. Heat Mass Transf. 2017, 107, 925-933.
- [31] B. Maciejewska, K. Strąk, M. Piasecka, *The solution of a two-dimensional inverse heat transfer problem using the Trefftz method*. Procedia Eng. 2016, 157, 82-88.
- [32] D. Murio, *Solution of inverse heat conduction problems with phase changes by the mollification method*. Computers and Mathematics with Applications, 24, pp. 45-57, (1992).
- [33] M.R. Shahnazari, A. RoohiShali, A. Saberi, *Solving inverse heat conduction problems by using Tikhonov regularization in combination with the genetic algorithm*, Adv. Mech. Eng. 13(2021) 211-220.
- [34] T. C. Smith, *A finite difference method for a Stefan problem*, Calcolo, vol 18, pp. 131-154, (1981). <https://doi.org/10.1007/BF02576493>
- [35] J. A. Rad, K. Rashedi, K. Parand, et al. *The meshfree strong form methods for solving one dimensional inverse Cauchy-Stefan problem*, Engineering with Computers, 33 pp. 547-571, (2017).
- [36] R. Reemtsen and A. Kirsch, *A method for the numerical solution of the one-dimensional inverse Stefan problem*, Numerische Mathematik, 45, pp. 253-273, (1984)
- [37] P. C. Rosenbloom and D.V. Widder, *Expansions in terms of heat polynomials and associated functions*, Trans. Amer. Math. Soc., 92 (1959), pp. 220-336.
- [38] L. I. Rubinstain, *The Stefan problem*, American Mathematical Society, Providence, RI, (1971).
- [39] E. Trefftz, *Ein Gegensruek zum Ritz'schen Verfahren*, in: Proceedings 2nd International Congress of Applied Mechanics (Zurich), pp. 131-137, (1926).
- [40] L. Vrankar, E.J. Kansa, G. Turk, F. Runovc, *Solving One-Dimensional Moving-Boundary Problems with Meshless Method*, Appl. Numer. Math. 53(2008) 1012-1031.
- [41] C. Wang, F. Wang, Y. Gong, *Analysis of 2D heat conduction in nonlinear functionally graded materials using a local semi-analytical meshless method*, AIMS Mathematics, 6(11) (2021), 12599-12618.
- [42] D. V. Widder, *Series expansions of solutions of the heat equation inn dimensions.*, Ann Mat Pura Appl Ser 4 1961, 55, pp. 389-409.
- [43] D. V. Widder, *Analytic Solutions of the Heat Equation*, Duke Math. J., V. 29, pp. 497-503, (1962).
- [44] D. V. Widder, *The role of the appell transformation in the theory of heat conduction*, Transactions of the American Mathematical Society, 109, (1) (1963), pp. 121-134.
- [45] D. V. Widder, *Expansions in series of homogeneous temperature functions of the first and second kinds.*, Duke Math. J., V. 36, pp. 495-510, (1969).
- [46] D.V. Widder, *The heat equation*, New York, San Francisco, London: Academic Press (1975).
- [47] H. Yano, S. Fukutani, A. Kieda, *A boundary residual metod with heat polynomilas for solving usteady heat conduction problems*. J. of the Franklin Inst., Vol 316, no. 4, pp. 219-298, (1983).
- [48] N. Zabararas, Y. Ruan, *A deforming finite element method analysis of inverse Stefan problems*, International Journal for Numerical Methods in Engineering, vol 28, pp. 295-313, (1989). <https://doi.org/10>
- [49] B. Zhang, G. Wu, Y. Gu, X. Wang, F. Wang, *Multi-domain physics-informed neural network for solving forward and inverse problems of steady-state heat conduction in multilayer media*, Phys. Fluids 34 (2022) 116116.

SDU UNIVERSITY, DEPARTMENT OF MATHEMATICS, ALMATY, KAZAKHSTAN
Email address: `narbekov.o@gmail.com`

ASTANA IT UNIVERSITY, DEPARTMENT OF COMPUTATIONAL AND DATA SCIENCE, ASTANA, KAZAKHSTAN
Email address: `samat.kassabek@astanait.edu.kz`

KAZAKH BRITISH TECHNICAL UNIVERSITY, INSTITUTE OF MATHEMATICS AND MATHEMATICAL MODELING,
NARXOZ UNIVERSITY, ALMATY, KAZAKHSTAN
Email address: `targyn.nauryz@gmail.com`